

Indian Head Division  
Naval Surface Warfare Center  
Indian Head, MD 20640-5035

---

IHCR 98-67  
31 July 1998

# AIR BLAST PROPAGATION INTO ACOUSTIC SHADOW ZONES

*J.W. Reed*

19990128 066

Approved for public release; distribution is unlimited.



# REPORT DOCUMENTATION PAGE

Form Approved  
QMB No. 0704-0188

Public reporting burden for this collection of information is estimated to average 1 hour per response, including the time for reviewing instructions, searching existing data sources, gathering and maintaining the data needed, and completing and reviewing the collection of information. Send comments regarding the burden estimate or any other aspect of this collection of information, including suggestion for reducing this burden, to Washington Headquarters Services, Directorate for Information Operations and Reports, 1215 Jefferson Davis Highway, Suite 1204, Arlington, VA 22202-4302, and to the Office of Management and Budget, Paperwork Reduction project (0704-0188), Washington, DC 20503.

1. AGENCY USE ONLY (Leave Blank)	2. REPORT DATE 31 July 1998	3. REPORT TYPE AND DATES COVERED Final Report	
4. TITLE AND SUBTITLE AIR BLAST PROPAGATION INTO ACOUSTIC SHADOW ZONES		5. FUNDING NUMBERS N00174-98-M-0177	
6. AUTHOR(S) J.W. Reed		8. PERFORMING ORGANIZATION REPORT NUMBER	
7. PERFORMING ORGANIZATIONS NAME(S) AND ADDRESS(ES) JWR, Inc. 5301 Central NE, Suite 220 Albuquerque, NM 87108		10. SPONSORING/MONITORING AGENCY REPORT NUMBER IHCR 98-67	
9. SPONSORING/MONITORING AGENCY NAME(S) AND ADDRESS(ES) Indian Head Division Naval Surface Warfare Center Indian Head, MD 20640-5035		11. SUPPLEMENTARY NOTES	
12a. DISTRIBUTION/AVAILABILITY STATEMENT Approved for public release; distribution is unlimited.		12b. DISTRIBUTION CODE	
13. ABSTRACT (Maximum 200 words)  Open burn-open detonation rocket motor disposal explosions conducted at the Utah Test and Training Range of Hill Air Force Base are delayed until proper weather conditions are present. These nominal conditions are an eastward-directed sound velocity versus height gradient that refracts airblast upward, away from the ground. Such weather conditions generally attenuate airblasts propagated at ground level, cause minimal disturbance to their neighborhoods, and are usually acceptable to explosion testers. These types of noise propagations have, thus, been mostly ignored in studies of nuisance airblast propagations. However, there are some cases where attenuated propagations shadowed either by atmospheric refraction effects or by terrain barriers can be of concern. Consequently, this paper attempts to develop a better understanding of wave diffraction, scattering, or diffusion into such shadow zones.			
14. SUBJECT TERMS Open burn Open detonation Airblast propagation		15. NUMBER OF PAGES 40	
17. SECURITY CLASSIFICATION OF REPORT UNCLASSIFIED		16. PRICE CODE	
18. SECURITY CLASSIFICATION OF THIS PAGE UNCLASSIFIED	19. SECURITY CLASSIFICATION OF ABSTRACT UNCLASSIFIED	20. LIMITATION OF ABSTRACT SAR	

This page intentionally left blank.

---

---

## FOREWORD

The work discussed in this report was conducted by JWR, Inc., under contract to the Indian Head Division of the Naval Surface Warfare Center (purchase order N00174-98-M-0177). The work was funded by the Strategic Systems Program as a portion of the Poseidon C-3 second-stage rocket motor disposal operation at the Utah Test and Training Range, Hill Air Force Base in Ogden, UT.

Approved and released by:



K. Wayne Reed  
Director, Explosive Technology Applications Division

This page intentionally left blank.

---

---

**CONTENTS**

<i>Heading</i>	<i>Page</i>
Foreword .....	iii
Introduction .....	1
Background .....	1
Analysis Procedure .....	3
Upwind Results .....	3
Downwind Results .....	4
"Utah" Upwind Model .....	5
Comparison with BLASTO Modeling .....	6
Upwind Sound Velocity Structures .....	7
Downwind Sound Velocity Structures .....	7
Discussion .....	7
Comparison with PROPA-GATOR Results .....	8
Conclusions .....	9
Recommendations .....	9

This page intentionally left blank.

# AIRBLAST PROPAGATION INTO ACOUSTIC SHADOW ZONES

Jack W. Reed  
JWR, Inc.  
Albuquerque, New Mexico  
May 1, 1998

## INTRODUCTION

Most of the Poseidon motor disposal explosions, which are fired during the warmer months at Hill Air Force Base Range, west of Great Salt Lake, Utah, were fired in weather conditions with an eastward-directed sound velocity versus height *gradient* that refracted airblast upward, away from ground. Such weather conditions generally attenuate airblasts propagated at ground level, they cause minimal disturbance to their neighborhoods, and they are usually acceptable to explosion testers. These noise propagations have thus been mostly ignored in studies of nuisance airblast propagations. Problems of atmospheric refractive *enhancement* of airblast propagation, which can irritate the neighboring population and cause various degrees of cosmetic structural damage, had priority for resolution. On the other hand, there are some cases where *attenuated* propagations, *shadowed* either by atmospheric refraction effects or by terrain barriers, can be of concern. Consequently, a better understanding of wave diffraction, scattering, or diffusion into such shadow zones may be useful.

Poseidon-disposal explosions, equivalent to about 20-t (18-tonnes) TNT, were recorded by sound-level meter on Antelope Island, in Great Salt Lake, at 65 km range, almost due east from the firing site and WSW from Ogden.. During 1995, 39 shots were fired with recordings made at Antelope Island of 24 of them. During 1996, 32 events were recorded of the 44 total. These will be the subjects of this analysis.

## BACKGROUND

During Operation DOMINIC, atmospheric nuclear tests at Christmas Island in 1962, several megaton-class bursts were detonated at kilometer altitudes about 30 km southwest of that atoll. In the prevailing easterly trade winds and relatively unstable thermal-structured tropical atmosphere, airblast was propagated upwind toward the atoll within strong sound velocity versus height gradient conditions that bent blast rays upward away from the surface, as illustrated in **Figure 1**. Depending on specific wind and temperature conditions at firing time, some blast rays reached pressure gages operated on the atoll, where measured overpressures were very close to Standard explosion predictions from *ANSI S2.20-1983* [1]. In other cases with stronger gradients, however, the limiting ray just grazed the ocean surface short of gage distance. In these cases, airblast was attenuated to below Standard explosion expectations. Analysis of detailed ray plots showed that overpressures in this shadow zone, beyond the grazing point, decayed in inverse proportion to the square of distance into the shadow zone. Undistorted spherical propagation at such relatively low overpressures decays almost inversely with distance — to the first power.

These results were published in *Weapons Test Report WT-2057*, October 1963 [2], classified secret along with all megaton-class explosion test data, and nearly forgotten. Recent attempts to declassify this report under currently relaxed rules have been delayed because of some included shot yields which have, so far, only been given yield ranges in released listings.

Nevertheless, this propagation principle can be stated — without available and adequate documentation — and examined for validity in other explosion test results.

Four series of small explosion tests, of 1-kg, 8-kg, and 65-kg C-4 explosives, were conducted in 1994 - 1996 by the Norwegian Defense Construction Service, to examine the attenuating influence on airblasts propagated through European forests. Vertical arrays of weather instruments and airblast pressure gages were operated on 30-m towers for all tests. Two series were fired on flat terrain, two series on hilly terrain. Summer and winter (snow-covered) tests were conducted over each terrain type. The first series in June, 1994, and now partially analyzed, showed that airblast overpressure indeed decayed inversely with distance-squared, at 30-m tower-top height from the closest weather-dependent ray point at that height, in upwind propagations, as shown in **Figure 2**. Similar paths to lower tower gages passed through forest trees and were even further attenuated. Analyses of the winter series measurements of February, 1995, is scheduled to begin soon.

Thus, this shadow-zone propagation model appears to be valid over three orders of magnitude in wave frequency and *nine* orders of magnitude in explosion yield! But neither these Norwegian nor DOMINIC results can be applied directly to the most common problem of horizontal propagation from a *surface* burst where the co-altitude ray is at the source, and inverse-distance-squared overpressure decay clearly does *not* prevail along the entire path.

Empiricism from Project PROPA-GATOR, 2.3-, 45-, and 1134-kg (5-, 100-, and 2500-lb) TNT tests of weather-dependent airblast propagation at Cape Canaveral, Florida, in 1979 [3], showed that overpressure-distance *decay rate* increased with increased sound velocity decrease — as measured between the surface and atop a 154 m meteorological tower — from an approximate Standard explosion source near 2-kPa overpressure.

These results were incorporated into Program BLASTO© for weather-dependent airblast predictions [4], but there are conceptual difficulties from yield-scaling principles [5] that require scaling *all* dimensions, both horizontal and vertical, in proportion to the cube-root of explosion yield, while conserving sound velocity difference (not gradient) in raypath equations. The height at which the atmospheric sound velocity gradient should be established for yields other than those used in these tests could only be guessed. It was assumed in BLASTO that the effective decrease occurred at the yield-scaled height of 154 m above 100-lb TNT surface burst. But yield-scaling this height for very large explosions often reached altitudes with much greater sound velocity deficits from low temperatures, well beyond the “calibrated” range, about  $10 \text{ m s}^{-1}$ , from PROPA-GATOR results. Also, such deep atmospheric layers usually contained several significant changes in sound velocity gradient that produced a variety of potential raypath patterns.

Sound velocity structure and ray paths for a typical Utah Poseidon explosion event are shown in **Figure 3**. It was hypothesized that there should be some point along the limiting raypath, emitted horizontally at  $0^\circ$  elevation angle from a surface burst, as it was refracted upward through the atmosphere, that would have predictive utility as a *virtual* source — whether scattered, diffracted, or diffused — for the attenuated wave reaching ground at distance. Radiosonde balloon weather measurements (raobs) near the shot — in space and time — allowed

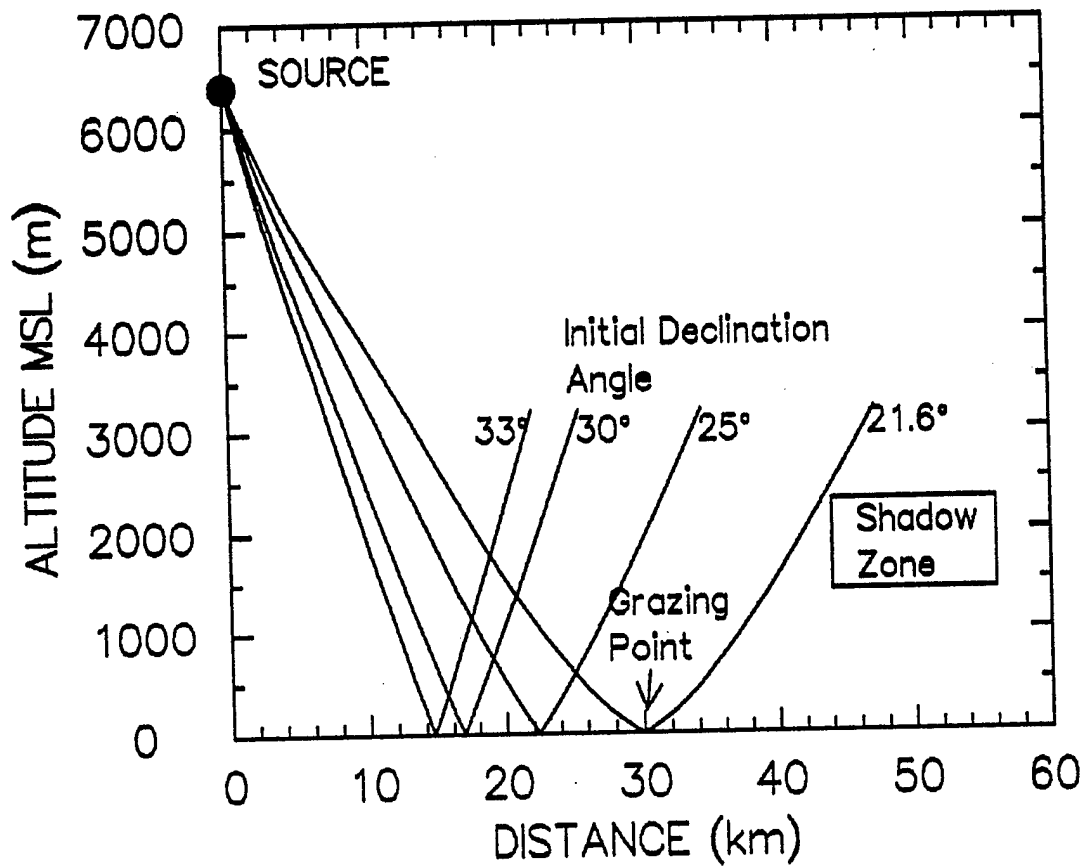


Figure 1. Explosion Ray Paths  
High-Altitude Bursts

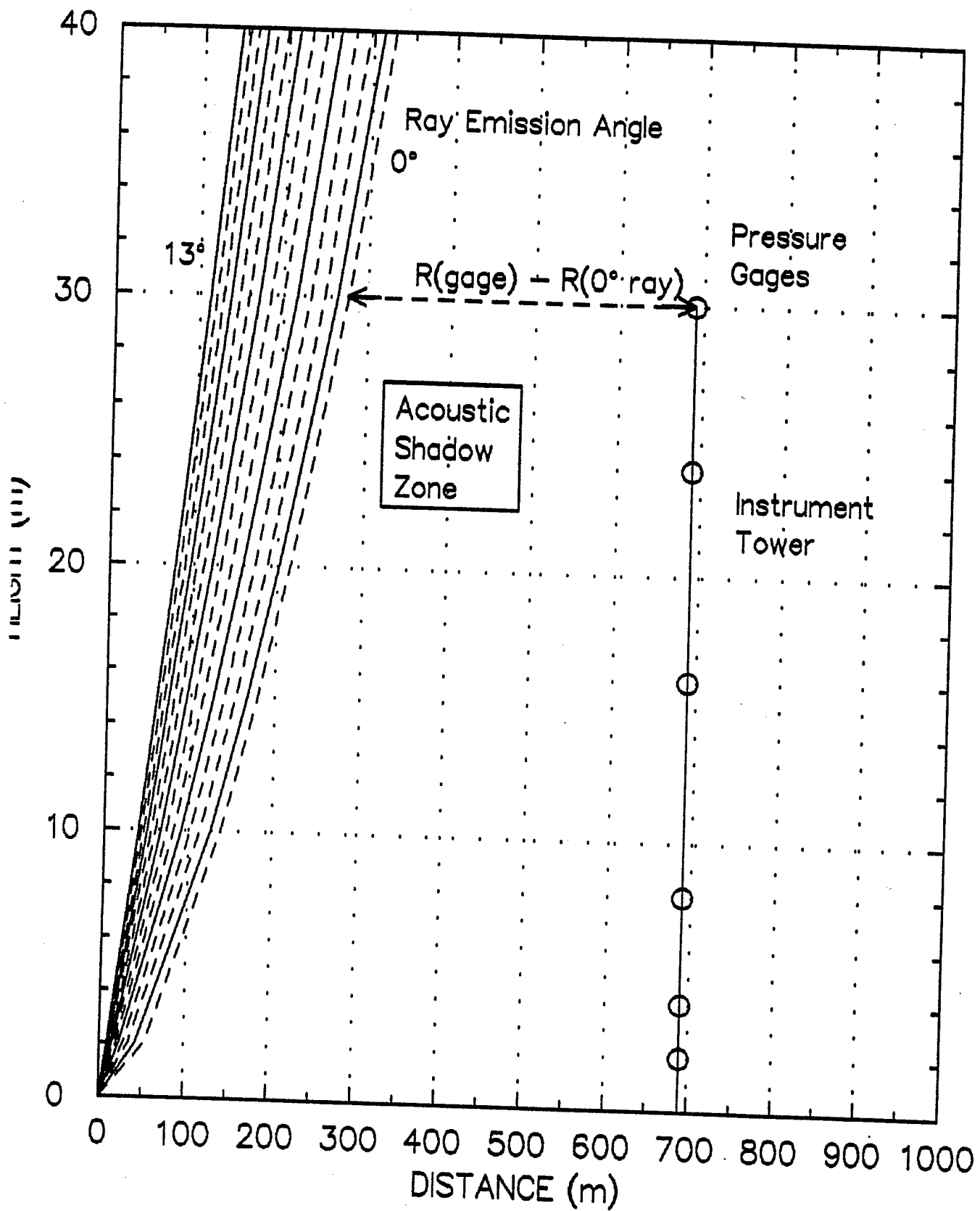


Figure 2. Upwind Raypaths, Norway Explosion Tests

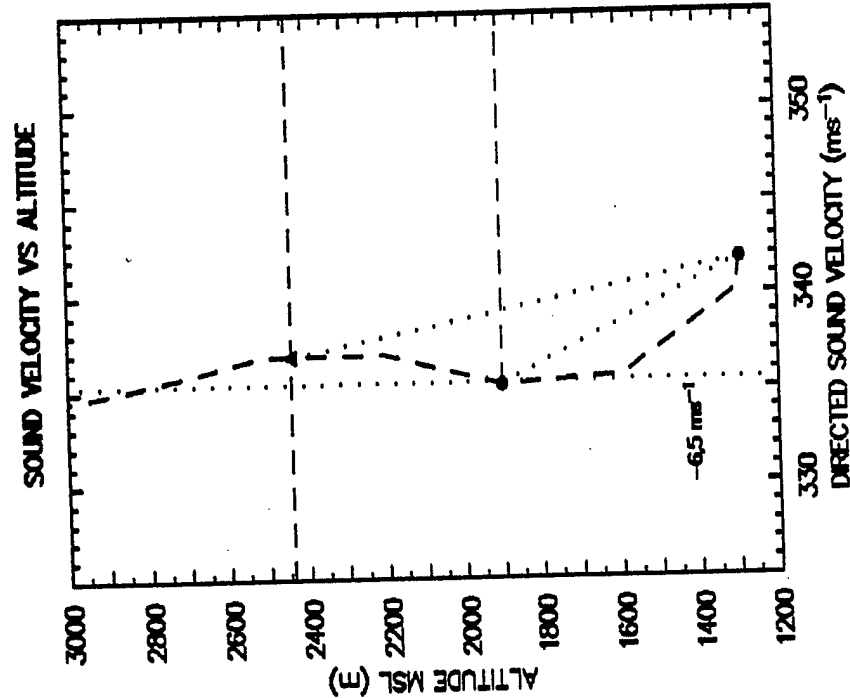
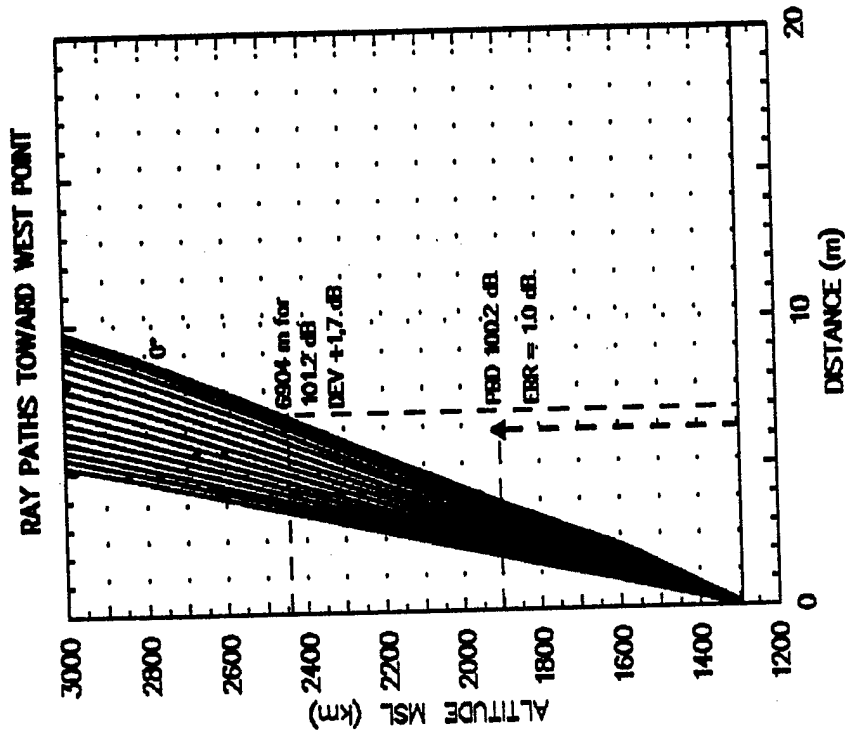


Figure 3. Poseidon Upwind Case, Raob #5036,  
4/26/95 2050 UTC

raypath calculations for distant propagations toward Antelope Island, as was shown in **Figure 3**. A first attempt to correlate measured overpressures with the limiting, horizontally emitted ray path proved quite successful, as will now be described.

## ANALYSIS PROCEDURE

1. At what distance from the explosion would a Standard explosion overpressure source be in order to decay with inverse-distance-squared to give the recorded overpressure? This answer is found on a Standard explosion log-log overpressure-distance curve, as shown by **Figure 4**, for a 17.9-Mg TNT surface-burst equivalent for two Poseidon motors. It is intersected by an inverse distance-squared line through the measured overpressure, shown as 110 dB (6.32 Pa) at 65 km, for example. Intersection occurs at 19.2 km with 72.9 Pa (126.5 dB). Such source distances are shown versus target decibel overpressures in **Figure 5**, for graphic solution. For the example in the right-hand graph of **Figure 3**, with a measured overpressure of 101.2 dB (2.3 Pa), this distance is 6904 m.

2. At that distance, what is the height of the raypath initially emitted at 0° elevation angle? BLASTO output tables of directed sound velocity versus height toward Antelope Island and West Point were used for calculating refracted paths for rays emitted at 1° increments up to 15° elevation angle, showing the altitude of the 0° ray at the specified distance as 2457 m MSL in **Figure 3**.

3. Considering the similarity yield-scaling problem, what is the non-dimensional *ratio* of this ray height above ground at 1293 m MSL to the gage distance? The limiting ray height, 1164 m, is divided by the 65 km gage distance to give the ratio 0.017906. These numerical values are shown in **Tables 1 and 2** for 1995 and 1996 events, respectively.

4. What is the *mean* sound velocity-height gradient below the limiting ray height? This is read from a BLASTO output table of sound velocities at the surface and at ray height; the difference was divided by the height to give the gradient,  $4.2696 \times 10^{-3} \text{ s}^{-1}$ , entered in **Table 1**. The connection is shown by a dotted line in the left graph of **Figure 3**. The dotted connection to the surface velocity reduced by  $6.5 \text{ ms}^{-1}$  at 1900 m MSL will be explained in a later section.

5. Is there any correlation between the distance ratio and this gradient, since upward ray curvature depends on gradient magnitude? The answer is **yes** — for events fired with *easterly* surface wind components and upwind propagations toward Antelope Island.

## UPWIND RESULTS

Correlated points, plotted in **Figure 6**, are scattered around a decadal diagonal line indicating roughly inverse proportionality. A statistical RMS fit line was only trivially different. Also, points from events in both 1995 and 1996 fell within the same belt, although there was larger scatter in 1996. Using the resultant relationship

$$Z/R = (10 G)^{-1} \quad (1)$$

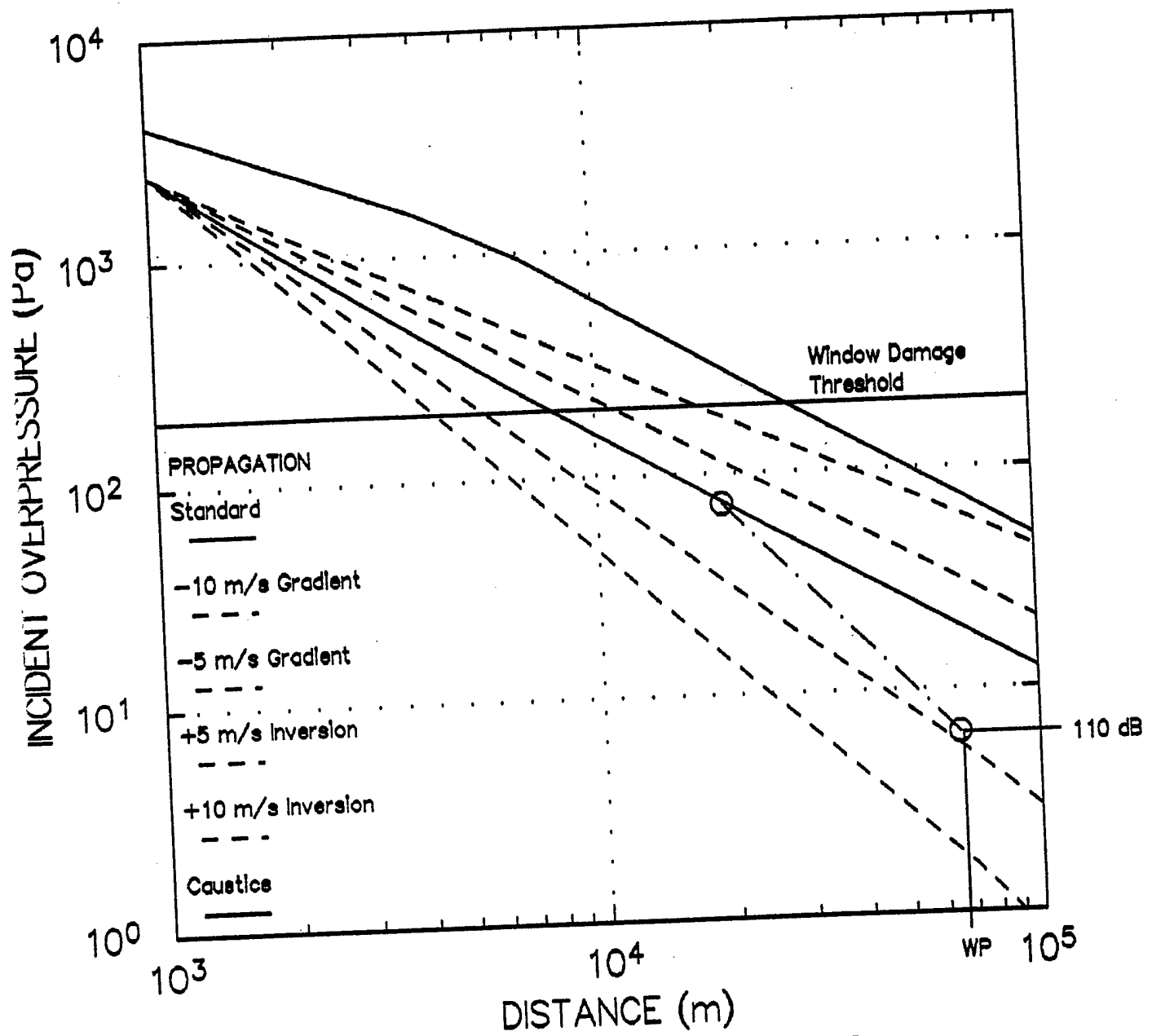


Figure 4. Overpressure-Distance Curves  
 POSEIDON Two-Motor Blasts  
 39,500-lb TNT Equivalent

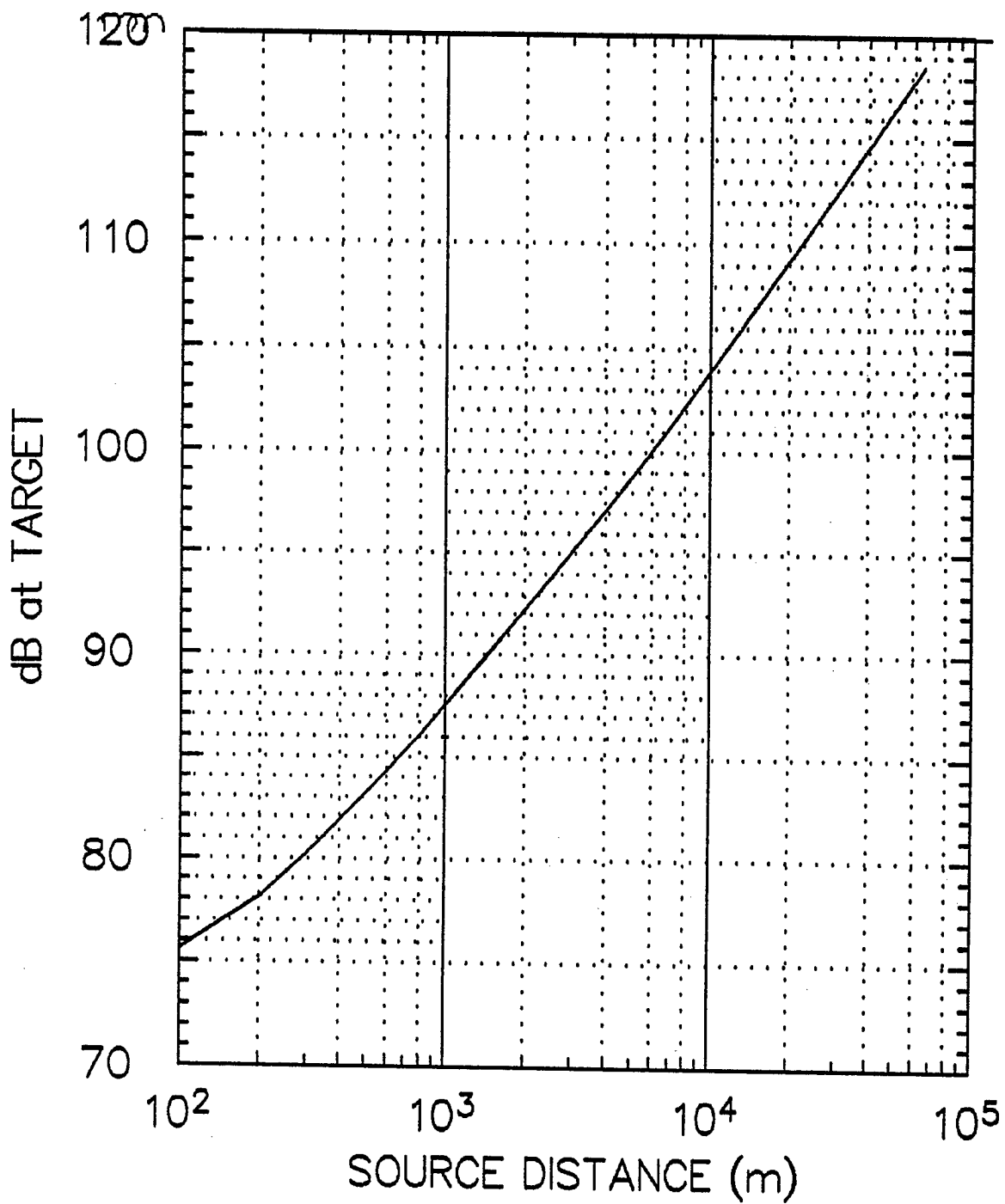


Figure 5. Overpressure (dB) vs Source Distance



Table 2. Shadow Zone Propagation Analysis, 1996.

Shot #	Date	Raob Time UTC	Raob #	Obsvd (dB)	Ray (°)	Ri (m)	MSL Zi (m)	AGL Zi (m)	100 x Z/R	1000 x Grad (s <sup>-1</sup> )	Duct Dpth (m)	Za (m)	Ra (m)	Model (dB)	Error (dB)	Down-wind?
456	4/1	2050	6015		0						0					No
459	4/4	1843	6018		7						10					Yes
463	4/8	1004	6021		0						0					No
466	4/11	1858	6024		12						10					Yes
470	4/15	2004	6028													
477	4/22	2057	6032		10											
478	4/23	2005	6036		6						3780					Focus
487	5/3	2018	6046		10						3536					Focus
491	5/6	1955	6050	118.5	2	65000					3824					Focus
494	5/9	1858	6054	100.6	5	6445	2266	946	1.4543	4.757	10	2687	7990	102.2	1.6	Yes
498	5/13	2003	6058	112.8	8	31576	10350	9030	13.8910	3.032	58	2274	7510	101.9	-10.9	Yes
505	5/20	2024	6064													
519	6/3	1852	6067	104.5	0	10801	3201	1881	2.8936	5.954	0	2412	7030	101.3	-3.2	No
522	6/6	1855	6070	98.6	2	4911	1855	535	0.8230	6.667	10	2295	7240	101.5	2.9	Yes
526	6/10	1827	6072	99.3	4	5413	1679	359	0.5523	5.392	224	2525	11000	104.6	5.3	Yes
528	6/12	1729	6075	99.5	0	5561	1945	625	0.9614	13.496	0	1802	4920	98.6	-0.9	No
529	6/13	1958	6079	105.5	0	12315	3854	2534	3.8981	2.586	0	3834	12200	105.4	-0.1	No
540	6/24	1919	6091	102.2	0	7900	2860	1540	2.3690	3.766	0	3046	8850	103.0	0.8	No
564	7/18	1843	6102	97.0	9	3943	1669	349	0.5369	7.965	10	2136	6970	101.2	4.2	Yes
568	7/22	1821	6108	102.4	0	8185	2675	1355	2.0844	3.542	0	3155	11300	104.8	2.4	No
570	7/24	1922	msg			7964										
571	7/25	1919	6111	113.4	1	34079	9620	8300	12.7681	2.241	10	4221	15300	107.2	-6.2	Yes
575	7/29	1926	6114	97.0	8	3900	1750	430	0.6615	9.070	10	2037	5520	99.3	2.3	Yes
577	7/31	1844	6118	97.0	0	3943	1988	663	1.0199	10.256	0	1954	3790	96.7	-0.3	No
578	8/1	1934	6122								0					No
584	8/7	1817	6128	91.8	0	1913	1666	356	0.5476	18.820	0	1665	1900	91.7	-0.1	No
585	8/8	1847	6131	106.5	0	14025	3883	2563	3.3427	2.458	0	3965	14300	106.6	0.1	No
589	8/12	1856	6134	108.2	0	17497	4503	3183	4.8965	3.864	0	3002	10600	104.4	-3.8	No
590	8/13	1936	6137	112.5	7	30393	10790	9470	14.5679	4.826	10	2667	8050	102.3	-10.2	Yes
592	8/15	2019	6141	97.2	0	4051	2023	703	1.0814	7.824	0	2151	4720	98.3	1.1	No
597	8/20	1912	6149	106.1	5	13319	3727	2407	3.7027	5.775	10	2446	8180	102.4	-3.7	Yes
599	8/22	1827	6152	97.8	0	5041	1907	587	0.9030	11.244	0	1898	5020	98.3	-0.5	No
603	8/26	1907	6155	84.9	0	1437	1506	186	0.2861	26.344	0	1567	1770	91.1	6.2	No
611	9/3	2111	6164	103.3	0	9500	3130	1810	2.7844	4.917	0	2642	7250	101.2	-2.1	No
613	9/5	2139	6167	110.5	9	24000	6430	5110	7.8608	1.722	10	5095	17300	108.0	-2.5	Yes
617	9/9	1920	6172	84.7	0	650	1396	76	0.1169	46.053	0	1461	1080	88.3	3.6	No
620	9/12	2014	6177	85.4	0	720	1390	70	0.1077	35.714	0	1502	1570	90.2	4.8	No
627	9/19	2023	6186	105.4	6	12000	2060	740	1.1384	2.568	10	3761	26800	111.0	5.6	Yes
631	9/23	2131	6193	102.0	0	6600	2442	1122	1.7260	2.585	0	3894	17800	108.2	6.2	No
638	9/30	2121	6206													
640	10/2	2041	6210	86.4	0	850	1442	122	0.1877	44.262	0	1467	982	87.4	1.0	No
641	10/3	2102	6213	96.7	7	3800	1665	345	1.0614	5.797	10	2451	8360	103.7	7.0	Yes
648	10/10	2149	6227	122.0	0	>65km										No
649	10/11	2201	6230	110.0	4	23000	4844	3524	5.4210	2.695	0	3742	18200	108.5	-1.5	Yes

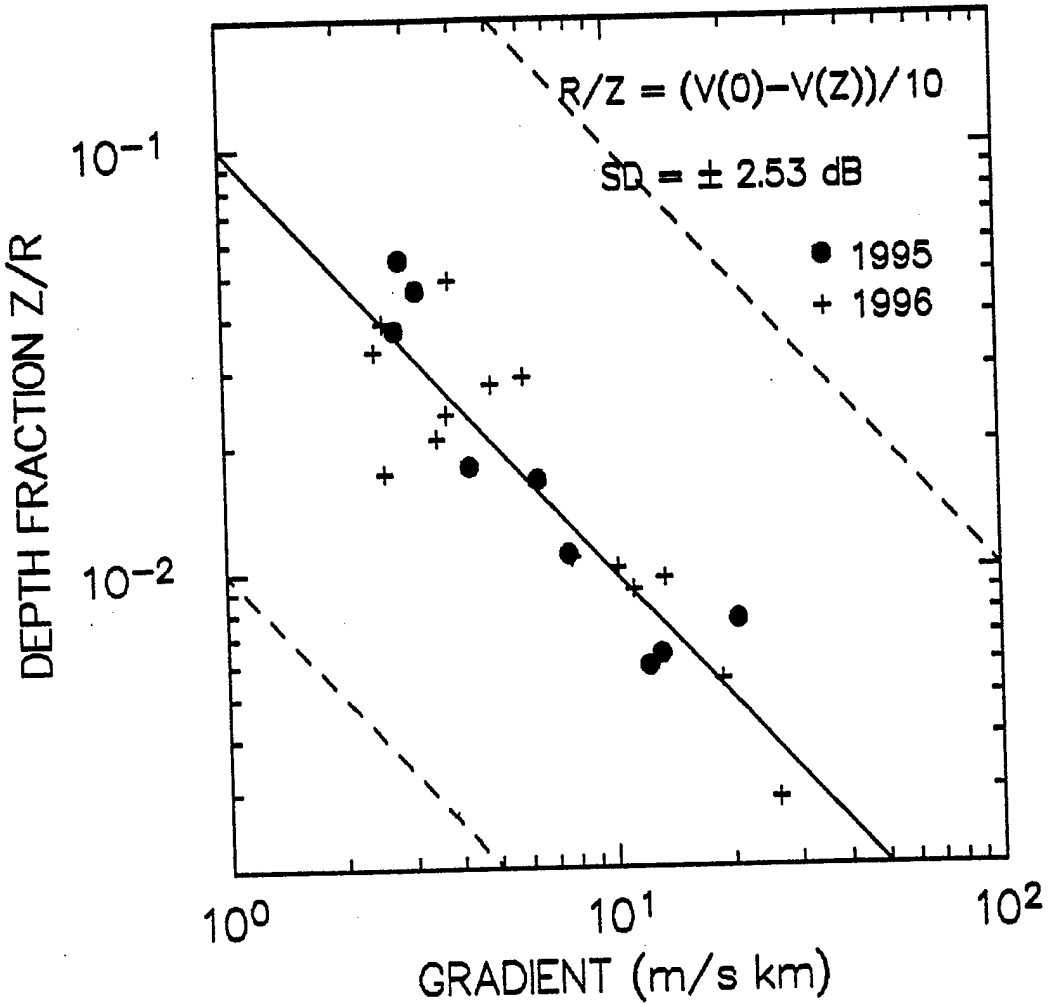


Figure 6. Depth Fraction vs Gradient – Upwind

where R is target distance, Z is the source height on the 0° ray, and G is directed sound velocity gradient, or decrease per *kilometer*. For each event, the depth fraction from Equation (1) was used to back-calculate a prediction for 65 km range. Comparison with observed overpressures showed an error standard deviation of  $\pm 2.53$  dB, or an error factor of  $(1.34)^{\pm 1}$  for 28 events.

These upwind errors are small for such great distance, considering the greater propagation variability found previously when comparing duplicate shots at short time separations [6], and attributed to atmospheric turbulence and mesoscale variability of winds aloft.

In what *appeared* to be an upwind case in **Table 1**, on 9/15/95, 114.8 dB was recorded, much above any expectation. Its source was calculated to be 40 km horizontally and over 9 km vertically from the burst, and above the highest raob reports. Thus this event could not be evaluated nor included in the error analysis. It must be assumed that some strong westerly winds were encountered along the raypath which were not encountered by the raob balloon, to cause such a strong wave.

Similarly, in another upwind case with an easterly flow near the surface, **Table 2** shows the *strongest* wave in two years of record, 122 dB was enhanced above Standard propagation on 10/10/96, and not explained by the raob weather report. In this case, an upper wind report of 238° 18.5 knots at 3300 m MSL must have missed an *effective* wind stream at least 7 knots stronger. That bang would have been quite loud at Antelope Island, but not approaching the window damage threshold of 200 Pa or 140 dB.

## DOWNWIND RESULTS

Explanation of propagations downwind from surface winds has proven less successful. Events fired with *westerly* surface wind components, however light, in **Figure 7** show much greater scatter and appear extremely sensitive to sound velocity gradient, which is hard to specify. Surface downwind ducting is assumed to extend only to the 10 m standard anemometer height, unless a higher-altitude raob measurement also showed an effective westerly wind component. These conditions should be expected to enhance eastward propagation in the surface frictional wind layer, *unless* the sound duct is blocked by terrain. And terrain did obstruct eastward propagation below about 20 m above these shot points, and before the airblast wave reached the flat lake surface.

Unfortunately, low-altitude details, reported as *significant* levels in original raob observations, were not included in delivered collections for dates prior to mid-August, 1995. These were apparently lost from computer files, so that only records at 1000-ft height increments were preserved. This resolution was all that was used for "BOOM-TOO" predictions [7] until the importance of low altitude details for these predictions was explained and 500-ft increments were adopted.

In those cases with surface wind ducting, the lowest ray that broke through the sound velocity inversion was used as the limiting ray for calculation and gradient correlation. These

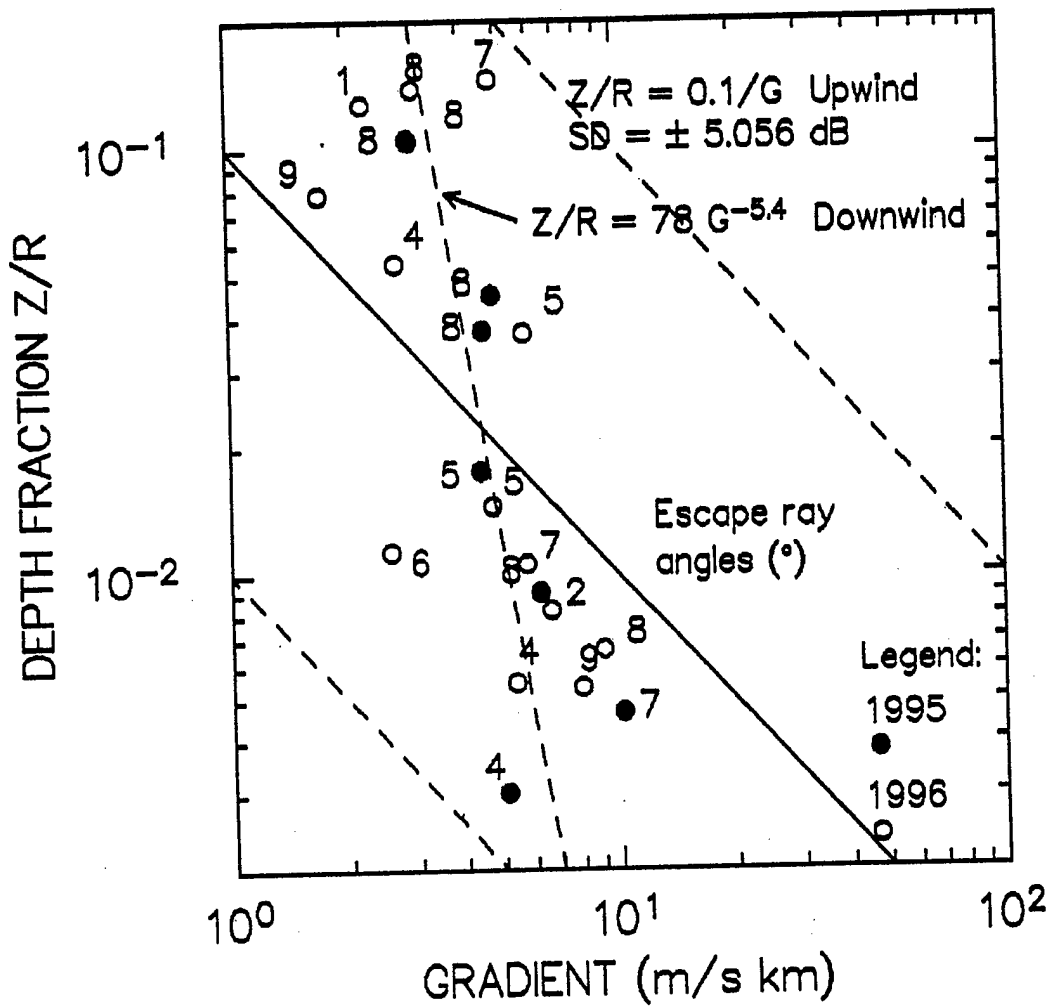


Figure 7. Depth Fraction vs Gradient – Downwind

escape ray angles are also entered in **Figure 7**, as well as an approximation line through the data points along

$$Z/R = 78.4 G^{-5.4} \quad (2)$$

Furthermore, as shown by **Figure 8**, there does not appear to be any correlation between this escape ray angle and the error from applying the upwind model of Equation (1) above the surface sound duct. Comparison with observed overpressures for the 22 cases showed a modeling error standard deviation of  $\pm 5.06$  dB, or an error factor of  $(1.79)^{\pm 1}$ , much larger than for upwind correlations.

### "UTAH" UPWIND MODEL

Calculations for acoustic ray paths through atmospheric layers with varying directed sound velocity are described by many references. An adequate method, derived from the Rayleigh approximation that the horizontal wind applies along the ray path, may be used for relatively horizontal propagations from explosions [8]. A more exact solution [9], using actual wind components along ray paths at larger elevation angles, is necessary for application to sonic booms and high-altitude explosions. The approximation method can be greatly simplified in the surface burst gradient case, for a *single* surface atmospheric layer, so that

$$X = Z [(V_0 + V_Z) / (V_0 - V_Z)]^{1/2} \quad (3)$$

Where X is horizontal and Z is vertical distance and V is directed sound velocity, subscripted 0 at the bottom and Z at the top of the layer. Interpretation of Equation (1) as  $(V_0 - V_Z) = 10^{-4} R$ , and approximating  $(V_0 + V_Z) = 2 V_0 = 680 \text{ ms}^{-1}$  the simultaneous solution is that

$$X = 2608 Z R^{-1/2} \quad (4)$$

Prediction for Antelope Island, at 65 km range, would thus proceed by identifying the altitude, Z, where  $(V_0 - V_Z) = 6.5 \text{ ms}^{-1}$ ; assuming that layer gradient was linear; calculating the source distance X; and finally reading the predicted pressure level from **Figure 5**. Similar predictions were made for cases with westerly surface winds, but using  $(V_i - V_Z) = 6.5 \text{ ms}^{-1}$ , where  $V_i$  is defined at the top of the low inversion. This procedure for upwind airblast predictions was dubbed the *UTAH Model*. Such predictions for Antelope Island in 1995 and 1996 are shown in **Tables 3** and **4**, respectively, along with their prediction errors.

Other predictions are also included in these two tables, including the BOOM-TOO method, which has apparently been required by agreement with the State of Utah for monitoring these events. BLASTO predictions were made, by this author (JWR), using the best obtainable weather data, and by NSWC-Dahlgren using the provided raob reports at 1000 ft and later at 500 ft height increments as shown in their CD-ROM report [10]. In BLASTO, when terrain profiles are provided, Standard overpressures are assumed in any terrain shadow, for lack of any better approximation. This probably is the source of most differences between JWR and NSWC BLASTO calculations.

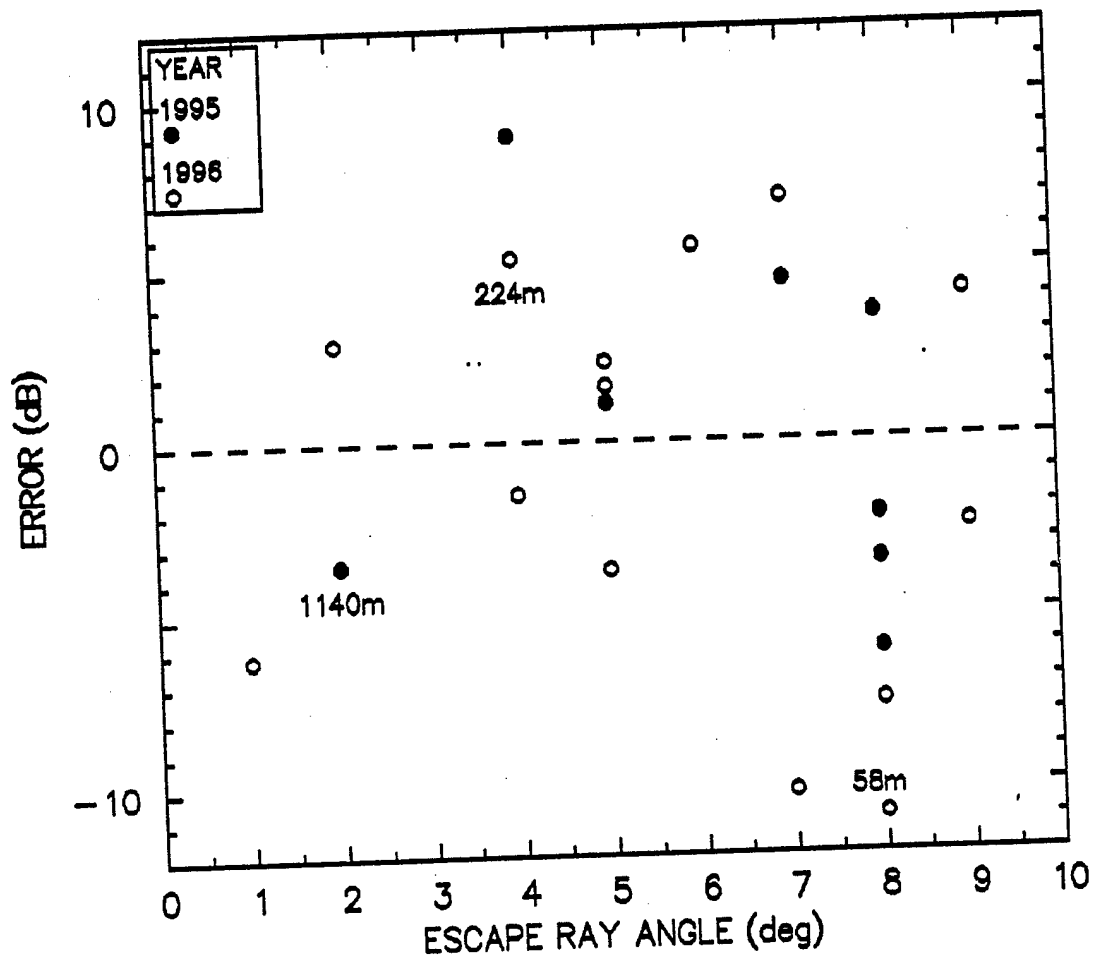


Figure 8. Prediction Error Versus Escape Ray Angle, Downwind Cases.  
 10-m Surface Wind Duct Except Where Depth is Indicated

**Table 3. Shadow Zone Predictions, 1995.**

1 Shot #	2 Date	3 Raob Time UTC	4 Raob #	5 Obsvd (dB)	6 Ray (°)	7 Duct Dpth (m)	8 Downwind ?	9 BLASTO JWR (dB)	10 BLASTO NSWC (dB)	11 UTAH MODEL (dB)	12 BOOM T00 (dB)	13-16 Prediction Errors (dB)			
												13 BLASTO JWR	14 BLASTO NSWC	15 UTAH MODEL	16 BOOM T00
94	4/5	2240	5020	118.8	15	100	Yes	119.8	118.2	113.7	125.5				
113	4/24	2105	5032	119.0	6	10	Yes	119.8	117.1	105.5	115.2	1.0		-5.1	6.7
115	4/26	2050	5036	101.2	0	0	No	106.0	102.8	100.4	120.1	0.8	-1.9	-13.5	-3.8
127	5/8	1800	5044	98.4	8	10	Yes	119.8	118.8	105.7	115.8	4.8	1.6	-0.8	18.9
137	5/18	1846	5049	117.8	7	10	Yes	119.8	117.7	103.3	112.4	20.4	20.4	-7.3	17.4
141	5/22	1847	5053	94.0	0	0	No	92.6	89.0	92.5	113.7	2.0	-0.1	-14.5	-5.4
150	5/31	1904	5057	96.3	4	10	Yes	119.8		105.0	112.1	-1.4	-5.0	-1.5	19.7
151	6/1	2015	5062		0	0	No	106.8		93.7	117.7	23.5		8.7	15.8
185	7/5	1906	5070	100.4	0	0	No	100.9		99.6	135.4	0.5		-0.8	35.4
205	7/25	2016	5095		0	0	No	103.3		78.0	126.1				
206	7/26	2032	5100		11	4500	Yes	119.8			121.8				
207	7/27	2046	5104		0	0	No	105.7		95.2	126.6				
211	7/31	2036	5107		0	0	No	98.5		99.0	115.4				
212	8/1	2049	5113		4	2500	Focus	131.8			128.2				
215	8/4	1924	5117		0	0	No	97.8		91.2	118.8				
218	8/7	2023	5123		9	10	Yes	119.8			114.2				
228	8/17	2055	5128		8	447	Yes	119.8			118.5				
229	8/18	2025	5133		0	0	No	95.3		84.4	126.9				
233	8/22	1824	5138		0	0	No	104.3			112.9				
235	8/24	2108	5144	111.5	8	10	Yes	119.8	118.9	104.3	113.6	8.3	7.4	-7.2	2.1
239	8/28	1928	5148		5	10	Yes	119.8			112.7				
241	8/30	1939	5152		0	0	No	103.5			118.7				
242	8/31	1840	5156	107.0	0	0	No	105.3	104.3	96.1	120.0	-1.7	-2.7	-10.9	13.0
247	9/5	2144	5161		10	10	Yes	119.8			121.2				
249	9/7	1948	5165		5	10	Yes	119.8			115.4				
250	9/8	1830	5168	93.9	7	10	Yes	119.8	118.3	106.0	120.0	25.9	24.4	12.1	26.1
254	9/12	1901	5172	93.6	0	0	No	107.0	105.5	105.2	112.4	13.4	11.9	11.6	13.9
256	9/14	1845	5176	108.4	0	0	No	100.6	97.7	100.6	111.9	-7.8	-10.7	-7.8	3.5
257	9/15	2002	5180	114.8	0	0	No	97.7	96.1	99.3	112.1	-17.1	-18.7	-15.5	-2.7
260	9/18	1910	5183	96.0	1	10	Yes	119.8	115.5	98.6	111.6	23.8	19.5	2.6	15.6
261	9/19	1825	5186	107.7	8	10	Yes	119.8	119.9	105.3	113.5	12.1	12.2	-1.4	5.8
263	9/21	2109	5192	97.0	0	0	No	105.0	102.3	99.4	121.4	8.0	5.3	2.4	24.4
267	9/25	2204	5198	115.9	2	1140	Yes	124.9	106.2	112.4	134.8	9.0	-9.7	-3.5	18.9
268	9/26	2015	5202	104.1	5	10	Yes	119.8	16.5	104.7	115.5	15.7	12.5	0.6	11.4
270	9/28	1931	5205	107.2	8	10	Yes	119.8	119.0	104.8	113.2	12.6	11.8	-2.4	6.0
274	10/2	1908	5209	111.6	16	8091	Focus	131.8	130.6		132.0	20.2	19.0		20.4
277	10/5	2006	5216	106.0	0	0	No	98.5		96.1	117.1	-7.5		-9.9	11.1
282	10/10	2001	5219	114.6	5	10	Yes	119.8	115.2	109.4	120.6	5.3	-4.5	-5.2	6.0
288	10/11	2044	5225	120.5	6		Yes	119.8	117.2	112.3	120.8	-0.7	-3.3	-8.2	0.3

Table 4. Shadow Zone Predictions, 1996.

1	2	3	4	5	6	7	8	9	10	11	12	13 14 15 16															
												Shot #	Date	Raob Time UTC	Raob #	Obsvd (dB)	Ray (°)	Duct Dpth (m)	Down-wind ?	BLASTO JWR (dB)	BLASTO NSWC (dB)	UTAH MODEL (dB)	BOOM TOO (dB)	Prediction Errors (dB)			
																								BLASTO JWR	BLASTO NSWC	UTAH MODEL	BOOM TOO
456	4/1	2050	6015		0	0	No	110.3			115.3																
459	4/4	2050	6018		7	10	Yes	119.8			111.6																
463	4/8	1904	6021		0	0	No	107.7			123.7																
466	4/11	1858	6024		12	10	Yes	119.8			111.5																
470	4/15	2004	6028								126.4																
477	4/22	2057	6032		10	3780	Focus	131.8			131.0																
478	4/23	2005	6036		6	3536	Focus	131.8			124.8																
487	5/2	2018	6046		10	3824	Focus	131.8			126.9																
491	5/6	1954	6050	118.5	2	4684	Focus	131.8	129.6	117.2	125.8	13.3	11.1	-1.3	7.3												
494	5/9	1858	6054	100.6	5	10	Yes	119.8				19.2															
498	5/13	2003	6058	112.5	8	58	Yes	119.8	118.0	104.4	112.7	7.0	5.2	-8.1	-0.1												
505	5/20	2024	6064				Focus	131.8	129.6		133.4																
519	6/3	1852	6067	104.5	0	0	No	106.6	105.8	106.0	117.7	2.1	1.3	1.5	13.2												
522	6/6	1855	6070	98.6	2	10	Yes	119.8	116.2	102.7	112.7	21.2	17.6	4.1	14.1												
526	6/10	1827	6072	99.3	4	204	Yes	118.4	115.9	105.3	114.0	19.1	16.6	6.0	14.7												
528	6/12	1729	6075	99.5	0	0	No	119.8	114.9	96.7	112.7	20.3	15.4	-2.8	13.2												
529	6/13	1958	6079	105.5	0	0	No	107.7	103.8	105.4	111.7	2.2	-1.7	-0.1	6.2												
540	6/24	1919	6091	102.2	0	0	No	102.3	100.1	104.4	121.7		-2.1	2.2	19.5												
564	7/18	1843	6102	97.0	9	10	Yes	119.8	120.8	105.8	115.3	22.8	23.8	8.8	18.3												
568	7/22	1821	6108	102.4	0	0	No	107.5	104.8	109.2	120.5	5.1	2.4	6.8	18.1												
570	7/24	1922	msg																								
571	7/25	1919	6111	113.4	1	10	Yes	119.8	115.4	101.0	115.2	6.4	2.0	-12.4	1.8												
575	7/29	1926	6114	97.0	8	10	Yes	119.8	119.1	104.0	114.9	7.4	22.1	7.0	12.9												
577	7/31	1842	6118	97.0	0	0	No	105.5	102.3	98.7	117.8	8.5	5.3	1.7	20.8												
578	8/1	1934	6122		0	0	No	109.1			120.4																
584	8/7	1817	6128		0	0	No	103.5	101.0	93.6	113.2	11.7	9.2	1.8	21.4												
585	8/8	1847	6131	106.5	0	0	No	103.9	101.7	102.3	127.0	-2.6	-4.8	-4.2	20.5												
589	8/12	1856	6134	108.2	0	0	No	105.9	104.3	105.0	116.9	-2.3	-3.9	-3.2	8.7												
590	8/13	1926	6137	112.5	7	10	Yes	119.8	119.0	98.1	112.1	7.3	6.5	-14.4	-0.4												
592	8/15	2019	6141	97.2	0	0	No	107.8	104.8	107.8	117.6	10.6	7.6	10.6	20.4												
597	8/20	1912	6149	106.1	5	10	Yes	119.8	116.2	104.8	113.7	13.7	10.1	-1.3	7.6												
599	8/22	1827	6152	97.8	0	0	No	103.5	94.4	100.3	116.8	5.7	-3.4	2.5	19.0												
603	8/26	1915	6155	84.9	0	0	No	86.6		95.6	111.9	2.1		6.1	27.0												
611	9/3	2111	6164	103.3	0	0	No	104.9	102.5	103.4	114.6	1.6	-0.8	0.1	11.3												
613	9/5	2139	6167	110.5	9	10	Yes	119.8	120.4	97.6	118.3	9.3	9.9	-12.9	7.8												
617	9/9	1920	6172	84.7	0	0	No	108.8	105.8	109.7	114.4	24.1	21.1	25.0	29.7												
620	9/12	2014	6177	85.4	0	0	No	107.7		107.0		22.3		21.6													
627	9/19	2023	6186	105.4	6	10	Yes	119.8	117.5	95.8	123.6	14.4	12.1	-9.6	18.2												
631	9/23	2131	6193	102.0	0	0	No	107.0	104.0	117.8	128.2	5.0	2.0	15.8	26.2												
638	9/30	2121	6206								113.7																
640	10/2	2014	6210	86.4	0	0	No	100.2	98.0	93.2	111.5	13.8	11.6	7.2	25.1												
641	10/5	2101	6213	96.7	7	10	Yes	119.8	117.7	103.3	110.9	23.1	21.0	6.7	14.2												
648	10/10	2149	6227	122.0	0	0	No	106.4	110.3	105.6	127.4	-15.6	-11.7	-16.4	5.4												
649	10/11	2201	6230	110.0	4	10	Yes	119.8	114.9	107.6	123.6	9.8	4.9	-2.4	13.6												

**Table 5. Statistical Summaries.**

**Gradient Propagation Analyses.**

	Number of Cases	Average Pressure (dB)	Standard Dev'n (dB)	Modeling Error(RMS) (dB)
UPWIND	28	99.99	8.654	2.531
DOWNWIND	26	107.14	8.120	5.056

**Prediction Error Comparisons**

	Upwind	Downwind	Total
BLASTO JWR vs NSWC	N=24	24	48
JWR	11.267	11.443	11.355
NSWC	9.666	9.718	9.692
BLASTO JWR vs UTAH	N=28	25	53
JWR	11.347	14.168	12.756
UTAH	9.602	8.431	9.069
BLASTO JWR vs BOOM-TOO	N=24	24	48
JWR	10.728	10.697	10.713
BOOM-TOO	18.939	18.775	18.860

Statistical prediction errors from these four methods are compared in **Table 5** from listings in **Tables 3** and **4**. First, comparing JWR BLASTO predictions with those by NSW, NSW predictions were slightly more accurate, by 21% in overpressure, in spite of their *not* having been made from more detailed raob reports. It appears, from this particular sampling, that weather and terrain details simply added confusion.

Comparing JWR BLASTO predictions with BOOM-TOO predictions demonstrated results from intrinsic fallacies in BOOM-TOO modeling, as previously described and criticized [11]. In an explosion experiment on Chesapeake Bay [12], measurements were used with an unfortunate selection for an empirical fitting function that precluded any realistic response to atmospheric enhancement of overpressures. This function was initially adopted in programming BOOM-TOO into an early digital mini-calculator for field use [7]. Overall, BOOM-TOO errors were 8.15 dB greater than BLASTO errors, which translates to a factor of 2.56 larger pressure prediction error.

The UTAH Model performed only a little better than BLASTO, which was surprising in light of the apparently good correlation that provided its foundation. Deviations from the assumed *single* gradient may obviously and strongly affect ray curvature, and thus the height and distance of the actual diffusive source for further  $R^{-2}$  propagation. When prediction errors are plotted against observed pressures in **Figure 9**, however, it clearly appears that low overpressures are overpredicted and high pressures are underpredicted by both BLASTO and UTAH.

Most remarkable and disturbing is that all errors, on average, are very nearly equal to the observation deviation from the sample mean. In other words, by simply predicting the *mean* value;  $UBAR = 99.99$  Pa, for each of 28 upwind propagations, an error standard deviation of only  $\pm 8.65$  dB resulted. This is 0.95 dB (12%) smaller than the UTAH model error. In 26 downwind cases, a larger  $UBAR = 107.14$  dB obtained, as could be expected, although the error standard deviation was smaller,  $\pm 8.12$  dB. That was 0.31 dB (4%) smaller than comparable UTAH model errors.

Compared to Standard overpressure at 65 km, 118.5 db, it shows 18.5 dB average excess attenuation for upwind propagation. About 1.3 dB of this may have been caused by atmospheric turbulence and classical atmospheric attenuation (molecular relaxation) [13], which has been ignored. It is not at all clear how this overall mean attenuation can be applied to generalized predictions that require yield scaling and do not have an archive of measurements for reference. Further data analyses may provide an appropriate value equivalent to the  $6.5 \text{ ms}^{-1}$  velocity decrease applied in UTAH predictions, but that is beyond the scope and capability of this report.

## COMPARISON WITH BLASTO MODELING

Gradient propagation pressure-distance curves used in BLASTO and derived from Project PROPA-GATOR results are shown in **Figure 10**, for 100-lb TNT surface bursts, and gradients of 5 and  $10 \text{ ms}^{-1}$ , as defined by the 154-m meteorological tower. UTAH calculations were made for gradients of 2, 5, and  $10 \text{ ms}^{-1}$  with the same dimensions, as shown by symbols on this figure. Reasonable ball-park agreement is shown, and at comparable yield-scaled distances

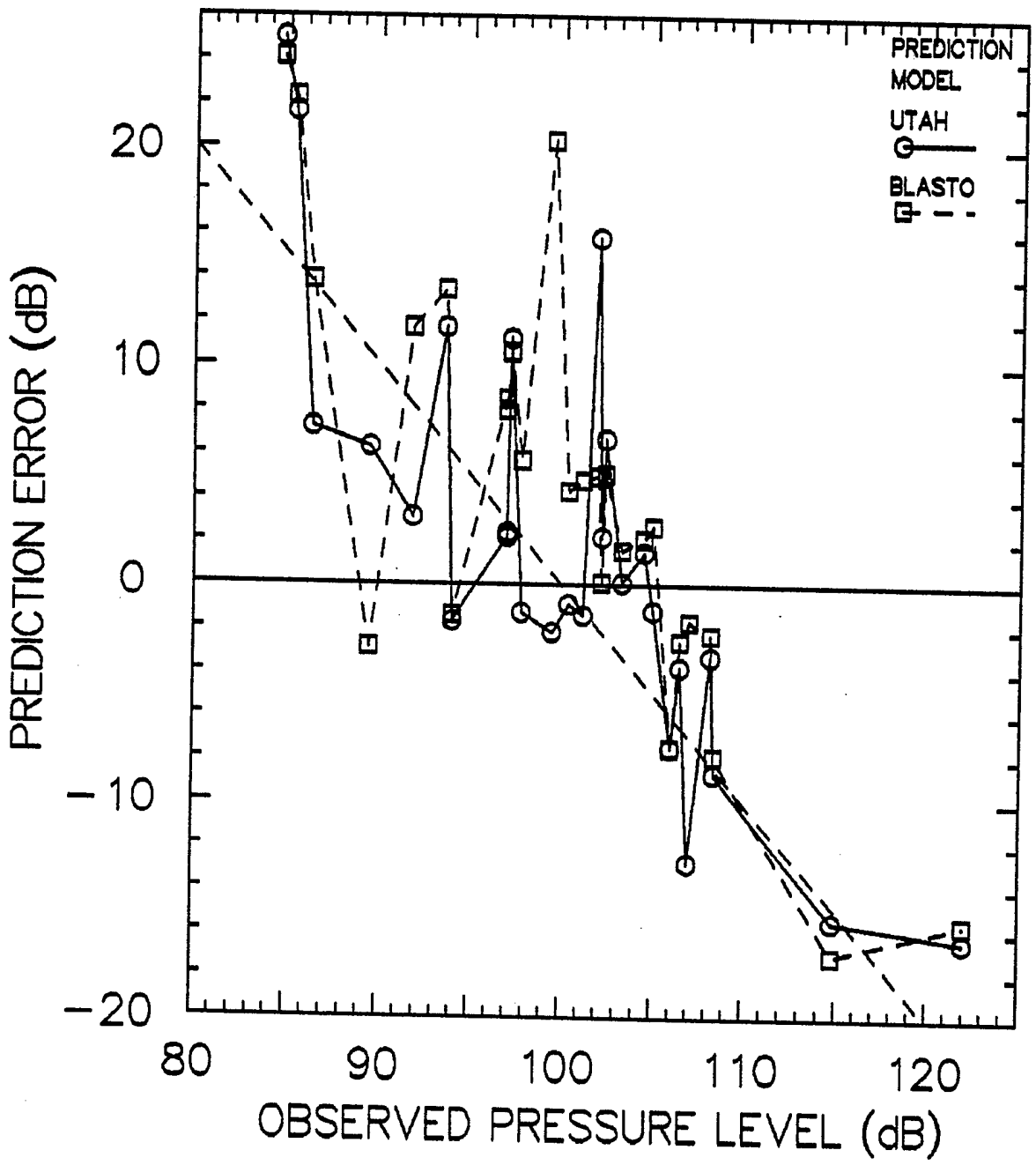


Figure 9. Prediction Errors, BLASTO and UTAH Models.

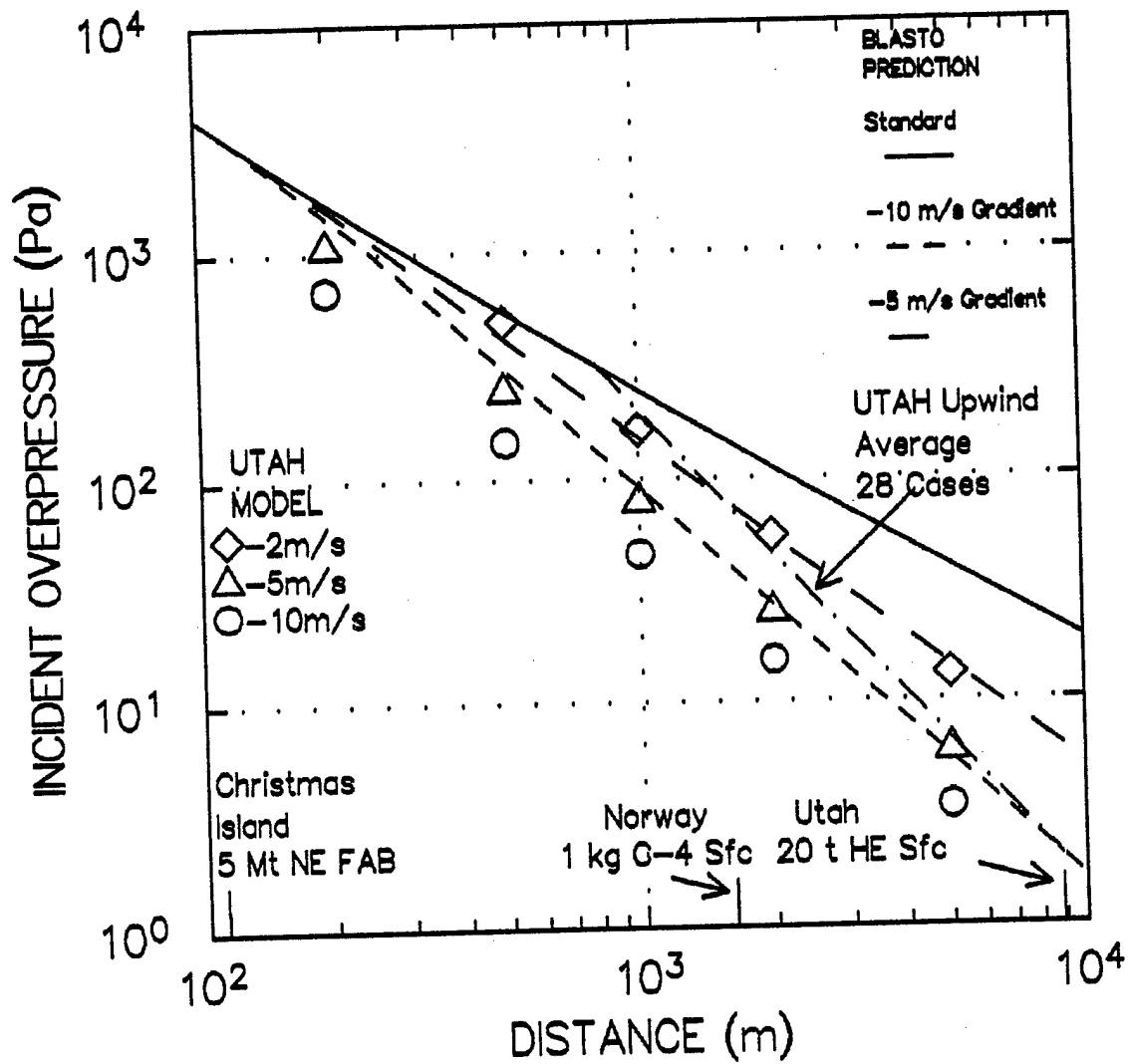


Figure 10. Gradient Model Comparison With PROPAGATOR 100-LB TNT Data

for both Norwegian tests and nuclear tests. Similarly, as shown by the dot-dash curve, the UBAR average prediction also crosses the same neighborhood.

### UPWIND SOUND VELOCITY STRUCTURES

In hope of finding additional clues to explaining error scatter in **Figure 6** and refining a prediction model, east-directed sound velocities were graphed. **Figure 11** shows ten cases with observed pressures from 89.5 to 100.4 dB; velocities for each raob were individually shifted so that the curve sequence from left to right across the figure represents increasing measured pressures. It was expected that gradients, as shown between surface and correlation height points, would become weaker with higher pressures (lessened upward refracted ray curvature), and this appears roughly confirmed for most cases. Two exceptions, #3 and #7, showed the greatest correlation point heights as well as the largest fitting errors. But there does not seem to be any clear identifying characteristic to their vertical structure that separates them from the other cases.

Similarly, **Figure 12** contains the other ten cases with higher observed overpressures, from 101.2 to 114.8 dB. This subset holds more examples with higher altitudes of correlation points, but the largest error magnitudes occurred with lower altitude points, in contrast to the pattern in **Figure 11**. Furthermore, the effective gradients in the two highest pressure cases, #19 and #20, are nearly the same as for #10 in **Figure 11**, at 10 dB lower pressure. In summary, these figures give no clear and obvious clues to correlation deviations.

The entire sequence of 20 upwind sound velocity structures is shown in **Figure 13** with heights marked on each for  $6.5 \text{ ms}^{-1}$  velocity decreases. The largest under-predictions shown in **Tables 3 and 4**, for #15, #17, #19, and #20, cluster in the lower right hand portion of the figure, while the largest over-predictions, for #3 and #7, fall in the upper left portion, further reflecting the conclusions from **Figures 9 and 11**.

### DOWNWIND SOUND VELOCITY STRUCTURES

Similarly, downwind sound velocities are shown in **Figure 14** for 93.9 to 111.5 dB pressures, and in **Figure 15** for pressures from 111.6 to 120.5 dB. Heights where  $(V_i - V_z) = 6.5 \text{ ms}^{-1}$  are marked, along with prediction error for each case. The only obvious pattern is the error trend with increasing overpressures that was displayed earlier in **Figure 9**. Detailed case studies of terrain blocking and surface wind ducting effects, using airblast measurements made on the shoreline and beyond the small ridgeline east of the shot area, may elucidate these propagations.  
sssddd

### DISCUSSION

Six explosions in 1995 and two in 1996 were measured at 114.8 to 122.0 dB, as shown in **Tables 1 and 2**, and close to the Standard explosion overpressure-distance curve. On 4/5/95 a westerly wind duct extended to 100 m above the terrain, according to detailed Raob #5020 winds and **Figure 15**, maintaining a near-Standard propagation. On 4/24/95 (Raob # 5032 in **Figure 15**)

- RAOB # dB
- 1. 6155 89.5
  - 2. 6128 91.8
  - 3. 5172 93.6
  - 4. 5053 94.0
  - 5. 6118 97.0
  - 6. 5192 97.0
  - 7. 6141 97.2
  - 8. 6152 97.8
  - 9. 6075 99.5
  - 10. 5070 100.4

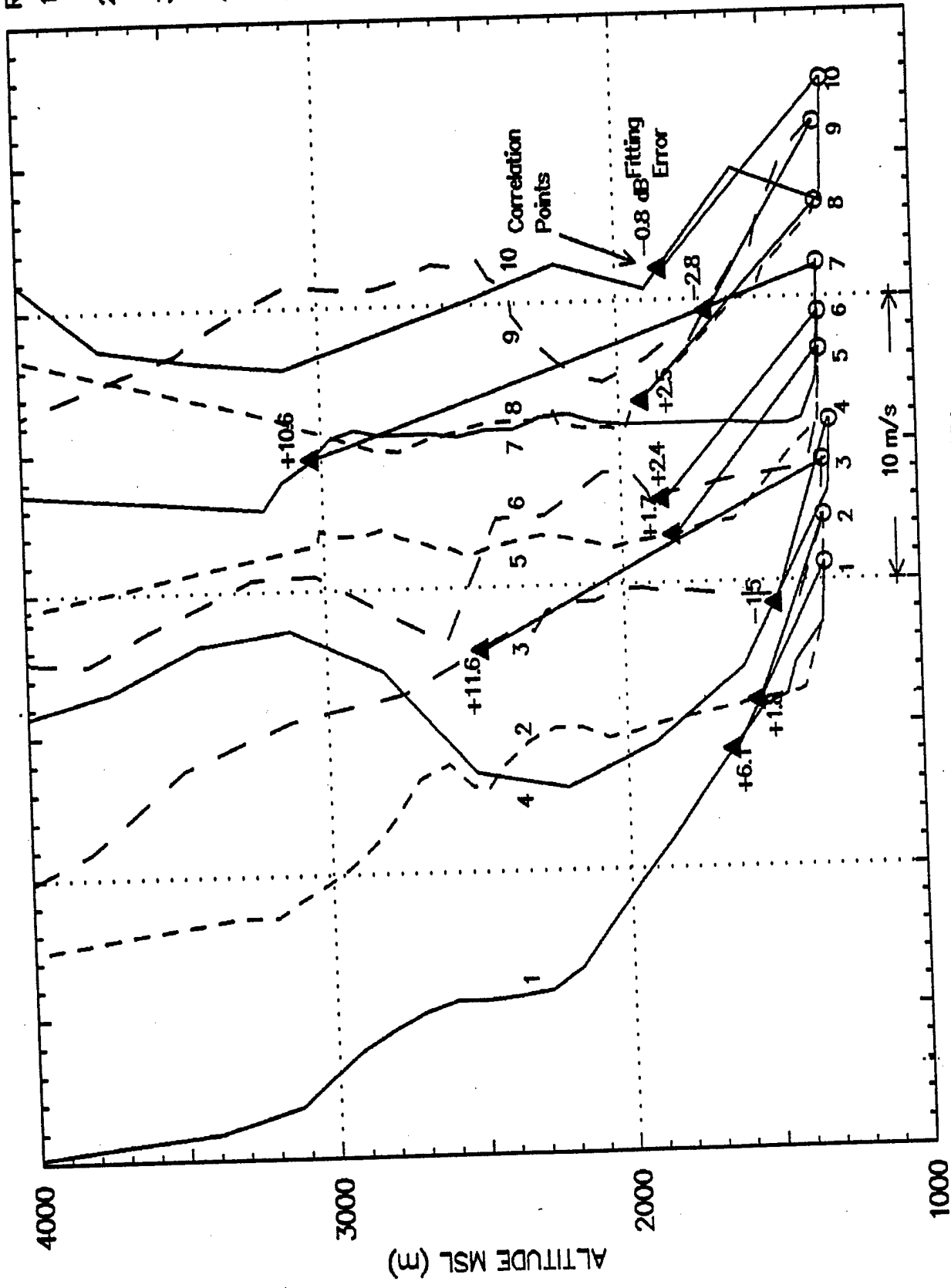


Figure 11. SOUND VELOCITY VS ALTITUDE, UPWIND CASES, 89.5-100.4 dB OBSERVED  
 Solid Triangles at  $V(0)-V(Z) = 6.5 \text{ ms}^{-1}$

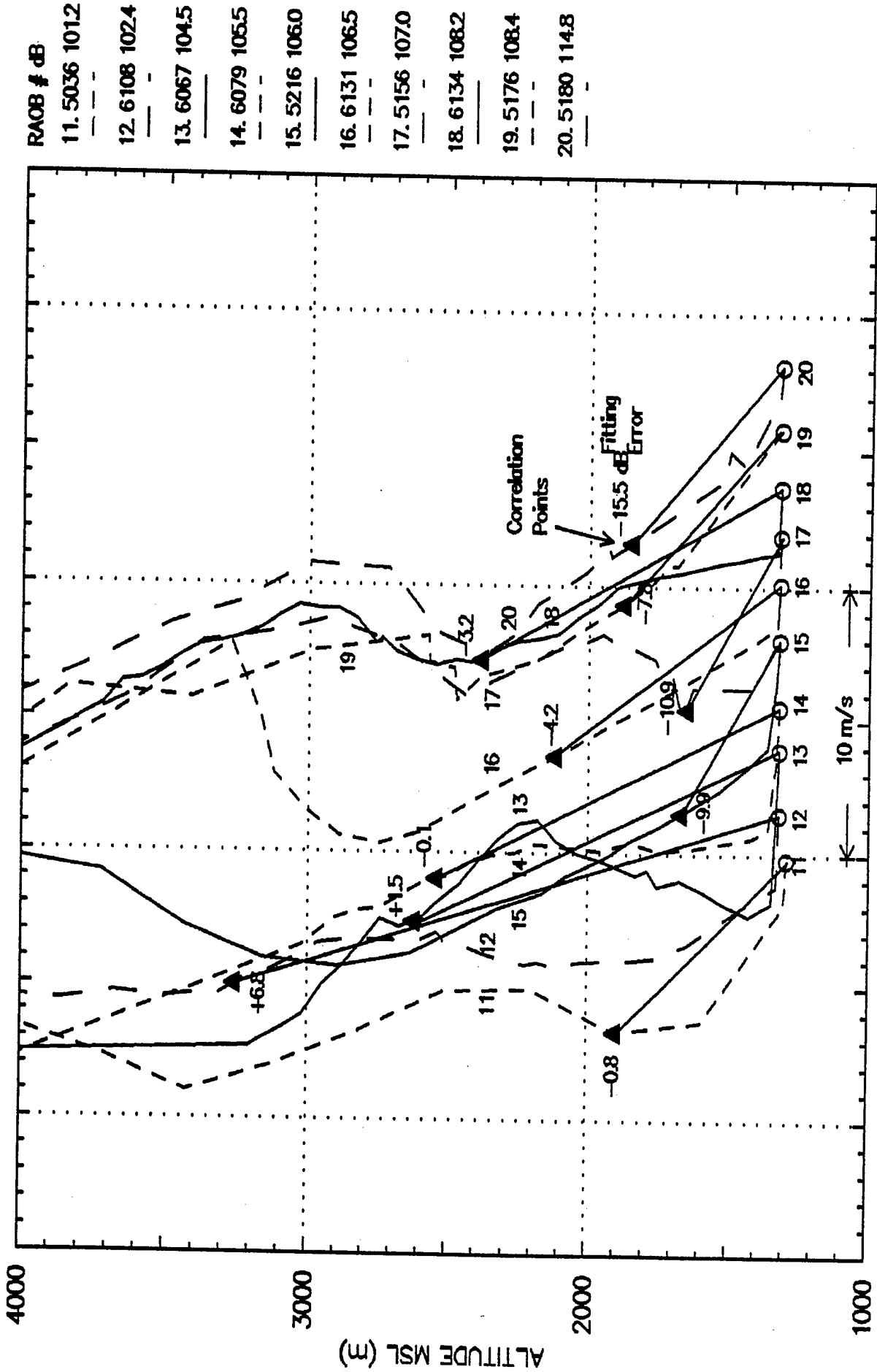


Figure 12. SOUND VELOCITY VS ALTITUDE, UPWIND CASES, 101.2-114.8 dB OBSERVED  
 Solid Points at  $V(0)-V(Z) = 6.5 \text{ ms}^{-1}$

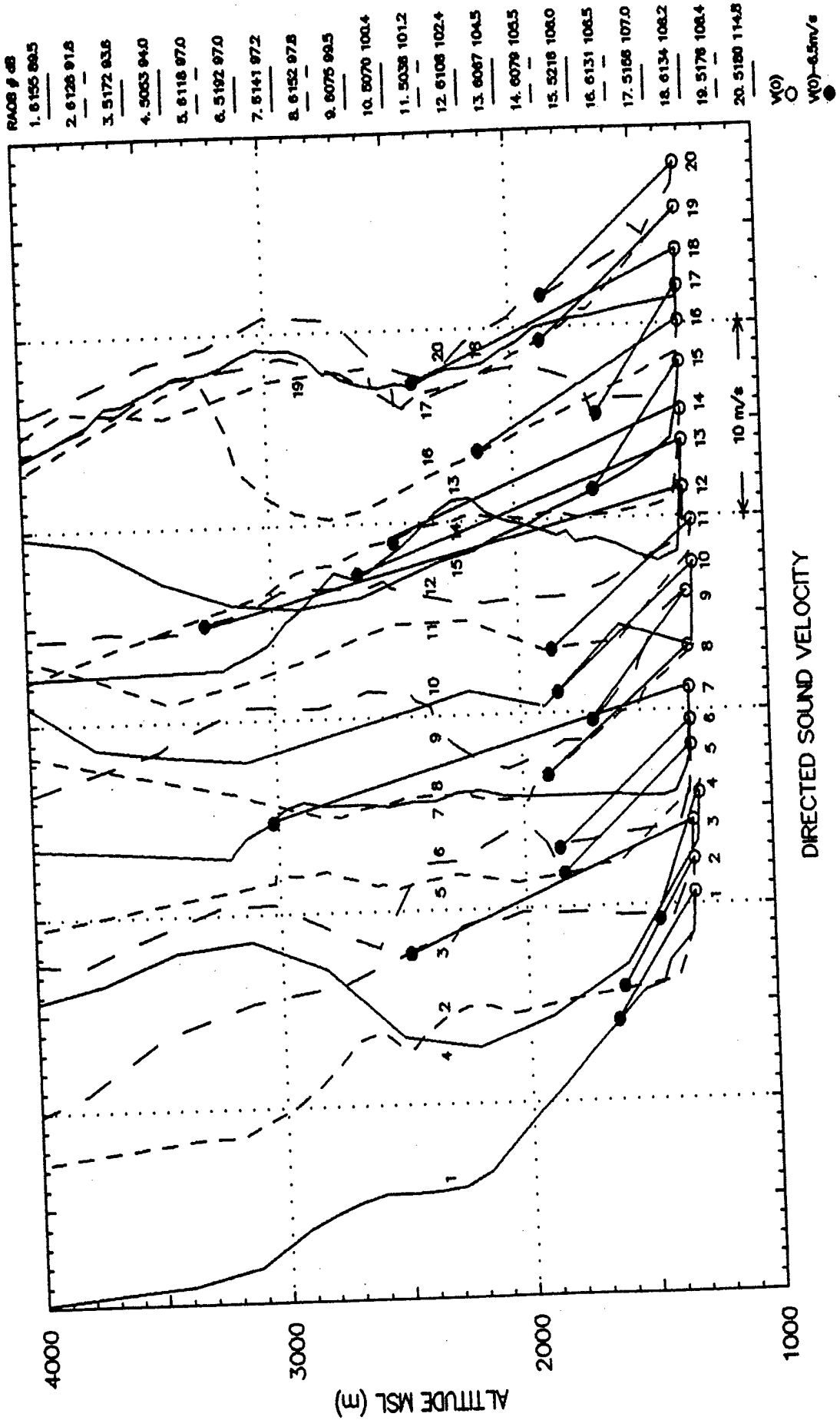


Figure 13. Sound Velocity vs Altitude, Upwind Cases.

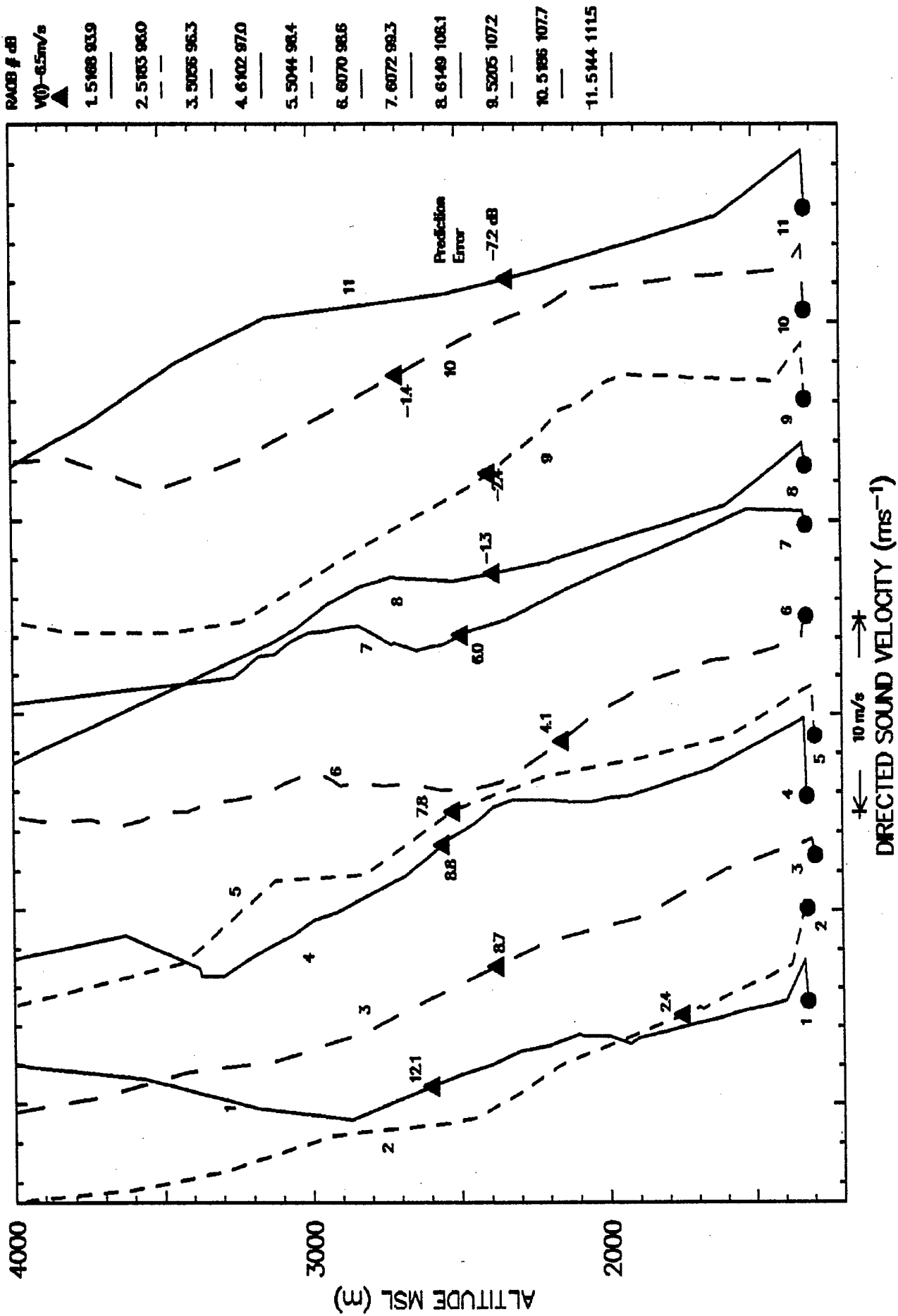
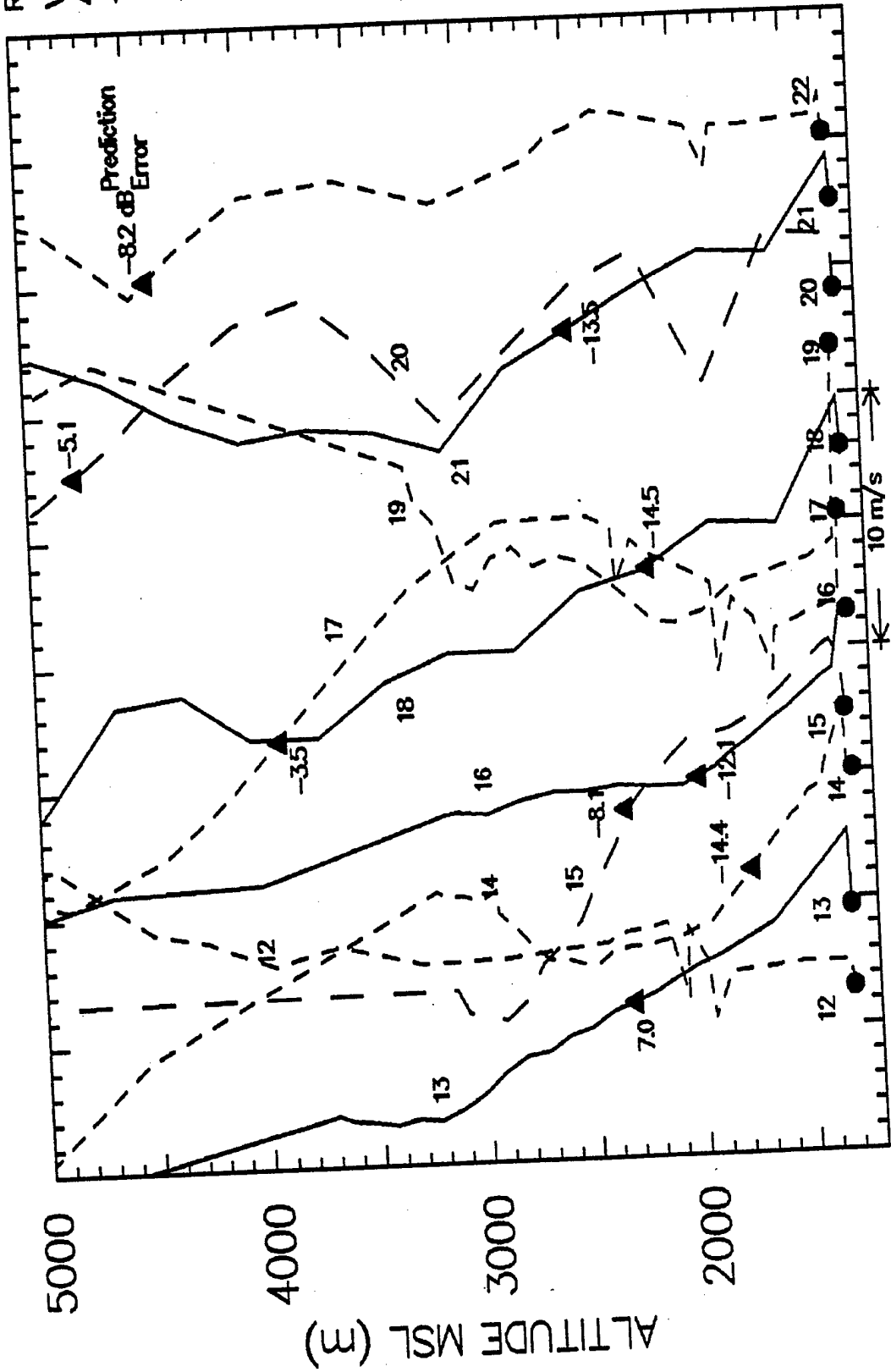


Figure 14. Sound Velocity vs Altitude, Downwind Cases, 93.9–111.5 dB

RAOB #	dB
V(1)	-6.5m/s
12	5209 111.6
13	6114 112.4
14	6137 112.5
15	6058 112.8
16	6111 113.4
17	5198 115.9
18	5049 117.8
19	6050 118.5
20	5020 119.8
21	5032 119.0
22	5225 120.5



DIRECTED SOUND VELOCITY (ms<sup>-1</sup>)

15. Sound Velocity vs Altitude, Downwind Cases, 111.6-120.0

and 5/18/95 (Raob #5049 in Figure 15), low-level wind details were not provided, but there must have been more than a shallow ground wind-friction duct at work, as occurred on 4/5/95. On 9/15/95 (Raob #5180, Figure 12) there was no indication, either at the surface or aloft, of westerly winds to propagate the observed overpressure, but they *must* have occurred along the true raypath but undetected by the raob balloon. It is quite likely that low-level wind circulations over Great Salt Lake differed from those over shot-site terrain where the raob was released. On 10/2/95 (Raob #5209, Figure 15) strong winds aloft showed several ducting layers up to 8 km MSL. This should definitely have been a NO-SHOOT condition. On 10/10/95 (Raob #5219) raob winds at 1500 m above ground came very close (by 0.1 m/s) to causing ducting so it can be safely assumed that some slightly higher wind speeds were encountered along the limiting raypath.

On 5/6/96 (Raob #6050, Figure 15), Standard propagation of 118.5 dB was observed from a dog-leg sound velocity curve extending up to 4700 m MSL, but with only  $0.1 \text{ ms}^{-1}$  excess aloft to generate a focused ray path. The Utah model only underpredicted by 1.3 dBA, so there was no strong focusing. Nevertheless, a small increase in the causal 38 knot wind at altitude could have ducted much more airblast energy, and its occurrence at a few hundred meters higher altitude could have moved the focused ground return to a greater distance toward Antelope Island or Ogden. Review of two earlier raob winds showed a slight speed reduction and southerly directional shift was occurring during the count-down, causing an encouraging trend to the velocity structure. But the go-ahead decision based on such small safety margins seems a bit hair-triggered.

On 10/10/96 (Raob #6227), sound velocity decreased very slowly with altitude, by only  $3 \text{ ms}^{-1}$  at 3000 m MSL, then to  $-6.5 \text{ ms}^{-1}$  by 3500 m MSL. Apparently, some winds along the ray path were stronger, causing this 50% overpressure amplification above Standard. There was, however, no marked dog-leg structure to threaten focusing.

## COMPARISON WITH *PROPA-GATOR* RESULTS

In Figure 10, of overpressure versus distance for 100-lb TNT surface bursts, one solid line shows Standard explosion propagation and two dashed lines that were fitted to *PROPA-GATOR* measurements at 200, 500, 1000, 2000, and 5000 m, for surface to 152 m tower-top decreases of  $-5 \text{ m/s}$  and  $-10 \text{ m/s}$  in sound velocity. These were calculated by the *BLASTO* program. Values were then calculated from the Utah model for comparison, as shown by symbols for  $-2$ ,  $-5$ , and  $-10 \text{ m/s}$ . The Utah model shows consistently lower predictions, although not many fell below *PROPA-GATOR* error scatter-bars. A dash-dot line connects the Utah data upwind average 99.99 dB measurement to the Standard overpressure curve following  $R^{-2}$  decay.

Also included in this figure are indicators of yield-scaled distances for Christmas Island nuclear tests, Norwegian kilogram tests, and Utah data at 65 km. All fall in the same general ball park of yield-scaled distances.

## CONCLUSIONS

It appears that explosion airblast propagation into acoustic shadow zones, hypothesized to follow inverse-distance-squared overpressure decay from nuclear megaton and chemical kilogram sources, also follows this decay from upwind measurements of Poseidon demolitions.

At this point it seems that the derived "Utah" model is superior to the PROPA-GATOR empiricism as applied by the BLASTO program, in that it evades yield-scaling problems and represents a much larger-scale experiment that should have allowed better measurement precision.

Using the Utah model for propagations downwind of low-altitude or surface winds also gave smaller prediction errors than BLASTO, although Utah downwind errors were also smaller than Utah upwind errors, for this particular sampling.

Standard deviations around the *mean* recorded overpressures, for 28 upwind and 26 downwind cases, were also smaller than UTAH prediction errors. But this would only provide predictive utility when a large number of similar previous events had been monitored.

On several occasions, shots were fired under marginal noise-propagation weather conditions. On a couple occasions, firings were conducted under conditions which could easily have caused focusing on the populated east side of Great Salt Lake.

## RECOMMENDATIONS

Case studies of the effects of the small terrain barrier, east of the firing point, on short range propagations to the lake shore could elucidate the surface downwind duct assumption, as it confused prediction and several times managed to transmit relatively strong airblast waves across Salt Lake.

The inverse-distance-squared model should be further explored to see if also applies in airblast shadows beyond other terrain barriers. Such study is scheduled for analyses of Norwegian test data from series conducted in hilly terrain. It also should be applied to measurements collected at Vandenberg AFB, in 1981, in a sequel to PROPA-GATOR, to determine the protection provided there by surrounding mountains.

The collection of Nevada nuclear test data contains many examples of gradient-dominated propagation to long distances of 50 to 150 km. These tests were mostly fired at early morning hours under strong desert night-time temperature inversions. But these inversion airblast ducts were blocked by 300- to 500-m mountains that surrounded both Yucca and Frenchman Flats. These data are in hand and could be analyzed against the Utah model.

## REFERENCES

1. American National Standards Institute, *Estimating Air Blast Characteristics for Single Point Explosions in Air, with a Guide to Evaluation of Atmospheric Propagation and Effects*, ANSI S2.20-1983 (R-1989), Acoust. Soc. Amer., New York NY, 1983.
2. Reed, J.W. and H.W. Church, "Blast Predictions at Christmas Island," Operation DOMINIC, Hazards Evaluation Unit Report WT-2057, Sandia Laboratory, Albuquerque NM, October 25, 1963.
3. Reed, J.W., "Project PROPA-GATOR Intermediate Range Explosion Airblast Propagation Measurements," *Min. 19<sup>th</sup> DOD Explosive Safety Seminar*, Los Angeles CA, 9-11 September 1980.
4. Reed, J.W., "Program BLASTO for Weather-Dependent Airblast Predictions," *Min. 24<sup>th</sup> DOD Explosive Safety Seminar*, St. Louis MO, August 26-31, 1990.
5. Glasstone, S. and P.J. Dolan, *The Effects of Nuclear Weapons, Rev. Ed.* U.S. Depts. Of Defense and Energy, Washington DC, 1977.
6. Reed, J.W., "Amplitude Variability of Explosion Waves at Long Range," *J. Acoust. Soc. Amer.*, 39, 5, 1, May 1966.
7. Douglas, D., "Blast Operational Overpressure Model (BOOM): An Airblast Prediction Method," AFWL-TR-85-150, Air Force Weapons Laboratory, Kirtland Air Force Base, NM, April 1987.
8. Cox, E.F., H.J. Plagge, and J.W. Reed, "Meteorology Directs Where Blast Will Strike," *Bull. Amer. Meteor. Soc.*, 35, 3, March 1954.
9. Thompson, R.J., "Ray Theory for an Inhomogeneous Moving Medium," *J. Acoust. Soc. Amer.*, 51, 1972.
10. Kordich, M.M. and D.A. Pollet, "UTTR Noise Abatement, 1995-1996 Data," CD-ROM Report NSWCDD TR-97/148, NSWC Dahlgren Div., Dahlgren VA, June 23, 1997.
11. Reed, J.W., "A Critique of Lorenz-Douglas Prediction Techniques for Weather-Dependent Airblast Propagations," ltr to G.Ullrich, HQ-DNA, Washington, DC, November 3, 1989.
12. Lorenz, R.A., "Noise Abatement Investigation for the Bloodworth Island Target Range: Description of Test Program and New Long Range Airblast Overpressure Prediction Method," NSWC TR 81-431, Naval Surface Weapons Center, Silver Spring, MD, 2 November 1981.
13. Reed, J.W., "Atmospheric Attenuation of Explosion Waves," *J. Acoust. Soc. Amer.*, 61, 1, January 1977.

## DISTRIBUTION

ADMINISTRATOR DEFENSE TECHNICAL INFORMATION CENTER ATTN DTIC-OCP 8725 JOHN J KINGMAN RD STE 0944 FT BELVOIR VA 22060-6218	1	US ARMY CONSTRUCTION ENGINEERING RESEARCH LABORATORY ATTN DR L L PATER 2902 FABER DRIVE CHAMPAIGN IL 61821	1
DIRECTOR STRATEGIC SYSTEMS PROGRAM ATTN CODE 27432 (W HELMRICH) 1931 JEFFERSON DAVIS HIGHWAY ARLINGTON VA 22241-5362	1	UTAH TEST AND TRAINING RANGE ATTN CODE 00 AL SUE (R. SHORT) 75TH SQUADRON HILL AFB UT 84406	1
COMMANDER DAHLGREN DIVISION NAVSURFWARREN ATTN G72 (KORDICH) 17320 DAHLGREN ROAD DAHLGREN VA 22448-5100	1	UTAH TEST AND TRAINING RANGE ATTN CODE 00 AL SE (T OLSEN) 75TH SQUADRON HILL AFB UT 84406	1
COMMANDER DAHLGREN DIVISION NAVSURFWARREN ATTN G72 (POLLET) 17320 DAHLGREN ROAD DAHLGREN VA 22448-5100	1	SIERRA ARMY DEPOT ATTN G LONG (BLDG 79) HERLONG CA 96113-5000	1
CHAIRMAN DOD EXPLOSIVE SAFETY BOARD ATTN DDESB-KT (WARD) 2461 EISENHOWER AVENUE ALEXANDRIA VA 22331-0600	1	JAYCOR ATTN DR P CHAN 9775 TOWNE CENTER DRIVE PO BOX 85154 SAN DIEGO CA 94551	1
CHAIRMAN DOD EXPLOSIVE SAFETY BOARD ATTN DDESB-KT (CANADA) 2461 EISENHOWER AVENUE ALEXANDRIA VA 22331-0600	1	COMPUTER SCIENCE CORPORATION UTAH TEST AND TRAINING RANGE ATTN R MITCHELL PO BOX 217 CLEARFIELD UT 84056	1
DIRECTOR DEFENSE SPECIAL WEAPONS AGENCY ATTN CODE LEE 6801 TELEGRAPH ROAD ALEXANDRIA VA 23310-3398	1	COMPUTER SCIENCE CORPORATION UTAH TEST AND TRAINING RANGE ATTN B DICKSON PO BOX 217 CLEARFIELD UT 84056	1
		COMPUTER SCIENCE CORPORATION UTAH TEST AND TRAINING RANGE ATTN J NELSON PO BOX 217 CLEARFIELD UT 84056	1

**Internal:**

950T	10
PME	3
600B	3
8230	1
840L	3